PROGRESS IN SCALE-RESOLVING SIMULATIONS WITH THE DLR-TAU CODE

A. Probst, S. Reuß

DLR, Institut für Aerodynamik und Strömungstechnik
Bunsenstraße 10, 37073 Göttingen, Deutschland

Abstract

This paper provides an overview of the recent development of scale-resolving simulation methods in the DLR-TAU code for flow simulations near the border of the flight envelope. On the numerical side, a hybrid low-dissipation low-dispersion discretization scheme is presented that allows for accurate wall-resolved and wall-modelled LES computations and is shown to provide satisfying hybrid RANS/LES predictions of a Delta wing flow on a unstructured mesh. In the field of physical modelling, the grey-area issue of non-zonal hybrid RANS/LES is addressed through a vorticity-sensitive sub-grid filter scale which is shown to improve the prediction of a backward-facing step flow. Moreover, an embedded-LES functionality based on the Synthetic Eddy Method is implemented in TAU and applied to a complex multi-element airfoil flow.

1. INTRODUCTION

The application of scale-resolving simulations, e.g., hybrid RANS/LES methods (HRLM) to aeronautical flows is driven by the demand for accurate predictions near and beyond the border of the flight envelope. However, while basic HRLM approaches are already suitable for massive separations, their applicability to more relevant flow phenomena like the onset of wing stall is still a challenge. Critical issues are for example the limited numerical accuracy of common aeronautical flow solvers when applied to scale-resolving simulations, and the so-called "grey area problem" [6], which describes a delayed onset of resolved turbulence at the HRLM interface.

This paper presents the progress that was achieved in the DLR project Digital-X on expanding the applicability range of such simulations with the unstructured DLR-TAU code [12] towards more relevant aeronautical flows. On the numerical side, a low-dissipation low-dispersion 2nd-order scheme (LD2-scheme, [5], [11]) for unstructured solvers has been developed and implemented in TAU. This scheme allows for accurate solutions of wall-modelled or wall-resolved LES and has been tested on a wide variety of flows, ranging from 2D-vortex transport problems [5] up to a 3D delta wing at high angles of attack.

The grey area at the HRLM interface has been addressed for 'non-zonal' methods that are suitable for strongly separated flows, as well as for 'embedded' approaches that are also suitable for attached or mildly separated flows. The latter methods require the introduction of synthetic turbulence at the hybrid interface, which has been realized by the implementation of the synthetic-eddy method (SEM, [1]). The improved prediction capabilities of these methods are demonstrated for different flow cases, including the multi-element DLR-F15 airfoil near stall.

2. BASIC SIMULATION METHOD

2.1. The Flow Solver DLR-TAU

The DLR-TAU code [12] is an unstructured compressible finite-volume solver for hybrid grids that may contain tetrahedral, hexahedral, pyramidal or prismatic elements. Incompressible flows can be simulated, too, by using low-Mach preconditioning (LMP). In its classic application as RANS (Reynolds-averaged Navier-Stokes) solver, TAU offers numerous turbulence models ranging from 1- and 2-equation eddy-viscosity models up to differential Reynolds-stress closures, which can further be coupled with methods to predict laminar-turbulent transition. Steady time integration is performed using either a semi-implicit lower-upper symmetric Gauss-Seidel (LU-SGS) method or a low-storage explicit Runge-Kutta scheme, both optionally coupled with multigrid of full approximation type. For time-accurate flow simulations, the implicit second-order dual-time stepping scheme is used.
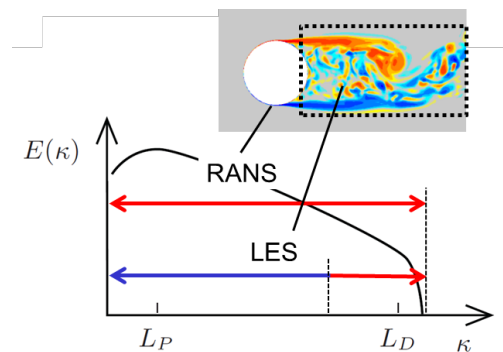

FIGURE 1. Turbulent energy spectrum with modelled (red) and resolved (blue) ranges for different simulation approaches.

2.2. Scale-Resolving Methods in TAU

Since the accuracy of classic RANS simulations is limited by the ability to model all effects of turbulent flow, there is a demand for methods that resolve (at least parts of) turbulence directly, such as Large-Eddy Simulation (LES). This is qualitatively explained with the help of the turbulent energy spectrum $E(\kappa)$ in FIGURE 1: While in RANS methods the whole spectrum (ranging from the production scale L_P to the dissipation scale L_D) is modelled

statistically, an LES is aimed to resolve the "large eddies" of turbulence both in space and time.

For high Reynolds numbers as usually faced in aircraft aerodynamics, TAU applies hybrid RANS/LES methods (HRLM). Their basic idea is to combine the advantages of conventional turbulence modelling (RANS) with turbulence-resolving methods (Large-Eddy Simulation, LES) in one unified simulation approach, see the cylinder flow in FIGURE 1. While RANS models provide reliable predictions of attached flows with low computational demand, they often fail in regions with strong separations. Such phenomena can be simulated more accurately with LES, which, however, imposes much higher requirements on the spatial and temporal resolution of the simulation.

Hybrid RANS/LES models such as the well-known Detached-Eddy Simulation (DES, [11]) aim to provide a sensible switching mechanism between RANS and LES depending on the local flow features (e.g., attached or separated flow) and grid properties. To this end, the length-scale variable in the equations of the underlying RANS model is replaced by a hybrid length scale l_{hyb}, which is basically a switching function between the original RANS length scale l_{RANS} (i.e., RANS mode) and an LES length scale l_{LES} that turns the hybrid model into a sub-grid scale model, suitable for Large-Eddy Simulation (i.e., LES mode):

(1) $\quad l_{hyb} = f(l_{RANS}, l_{LES})$ with: $l_{LES} = C_{DES} \cdot \Delta$

Here, Δ represents a grid-dependent local filter width, and C_{DES} is a model coefficient for calibrating the LES mode of the hybrid model. In classic DES, Δ is given by the maximum local cell spacing, $\Delta_{max} = max(\Delta_x, \Delta_y, \Delta_z)$.

The TAU code also provides more recent variants of DES like the Delayed DES (DDES, [15]) or the Improved Delayed DES (IDDES, [13]). While the former adds a "shielding" mechanism to safely keep attached boundary layers in RANS mode, the latter offers the alternative approach to resolve wall-bounded flow in the sense of a wall-modelled LES (WM-LES).

3. IMPROVED NUMERICAL SCHEMES

Irrespective of the modelling details, the accuracy of scale-resolving simulations is governed by numerical discretization errors, which can be classified as dissipation (amplitude errors) and dispersion (phase / wavelength errors). Although these errors diminish with finer grid spacing, the dependency of sub-grid LES models on the local grid spacing calls for numerical schemes that provide low discretization errors for any grid resolution.

3.1. Low-Dissipation Low-Dispersion (LD2) Scheme

To provide low discretization errors for scale-resolving simulations, a low-dissipation low-dispersion scheme, denoted as LD2 scheme, has been recently developed and implemented in TAU. It is based on a 2nd-order energy-conserving skew-symmetric convection operator that is combined with a minimal level of 4th-order artificial matrix dissipation for stabilization [9]. Moreover, the central flux terms employ an additional gradient extrapolation that effectively increases the discretization stencil and is used to reduce the dispersion error of the scheme [5].

Both ingredients are essential for accurate scale-resolving simulations of wall-bounded flows with the TAU code [11]. For illustration, consider the results of simulations of the plane channel flow in FIGURE 2 and FIGURE 3. They show the mean-velocity and Reynolds-stress profiles from wall-resolved LES computations that were obtained on a hexahedral grid with sufficient resolution to resolve turbulence down to the wall. While the original numerical scheme in TAU (denoted as "Reference scheme" or "Ref.") yields too large normalized velocities u^+ in the logarithmic layer (FIGURE 2) and also overpredicts the streamwise normal stress component (FIGURE 3), both the basic low-dissipation (LD) and the full (LD2) scheme vastly reduce the deviations from the reference DNS [7].
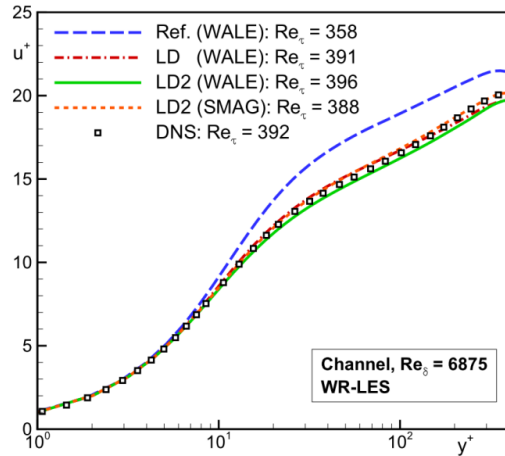

FIGURE 2. Non-dimensional mean velocity profile in the plane channel flow at $Re_\tau \approx 395$.
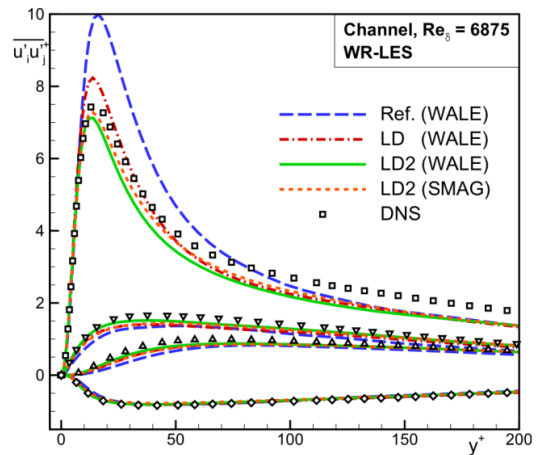

FIGURE 3. Non-dimensional resolved Reynolds stresses in the plane channel flow at $Re_\tau \approx 395$.

For a wall-modelled LES shown in FIGURE 4, which was run at a much higher Reynolds number ($Re_\tau \approx 4200$ instead of 395), but on an even coarser grid, the results with the new schemes in TAU are also satisfying. Here, the LD2 scheme yields a somewhat improved logarithmic behaviour near the RANS/LES interface compared to the basic LD scheme.
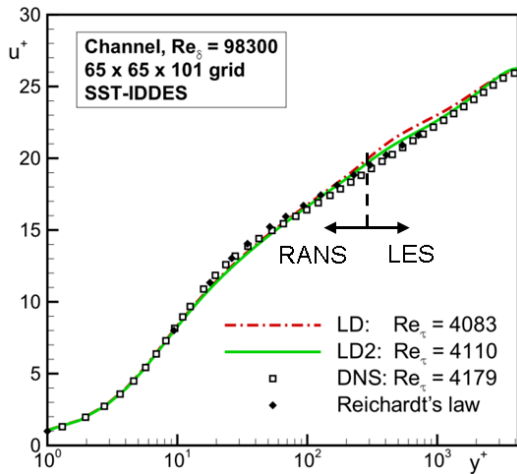
FIGURE 4. Non-dimensional mean velocity profile in the plane channel flow at $Re_\tau \approx 4200$.

3.2. Hybrid LD2 Scheme

For more complex geometries, the grids used in industrial practice may not meet the quality requirements for a stable application of the LD2 scheme in all areas. In particular, problems may arise from large (high-aspect ratio) cells near the farfield boundaries or skewed unstructured cells around geometric complexities.

For this reason, a hybrid LD2 scheme was developed, which allows a local blending of the numerical parameters Ψ of the LD2 scheme with the more conservative (i.e., more dissipative and dispersive) reference scheme:

$$(2) \quad \Psi = (1 - \sigma) \cdot \Psi_{LD2} + \sigma \cdot \Psi_{Ref}$$

The blending is controlled by the numerical weighting function σ by Travin & Shur [16], which discerns between the well-resolved vortex-dominated flow regions (where the LD2 scheme is active) and coarse-grid irrotational regions (where the Ref. scheme is active).

The functionality of the hybrid LD2 scheme is illustrated in FIGURE 5 for the DDES computation of a Delta wing at high incidence ($\alpha = 23°$). It shows an iso-surface of the Q-criterion to visualize the longitudinal-vortex system on the wing, which is coloured by the blending function $1-\sigma$. Red colour ($1-\sigma \approx 1$) indicates the use of the LD2 scheme. Although there are regions with $1-\sigma < 1$ in the initial shear layer at the leading edge and directly near the wing surface, the largest parts of the resolved vortical flow yields $1-\sigma \approx 1$, thus providing the low-dissipation low-dispersion discretization where needed.
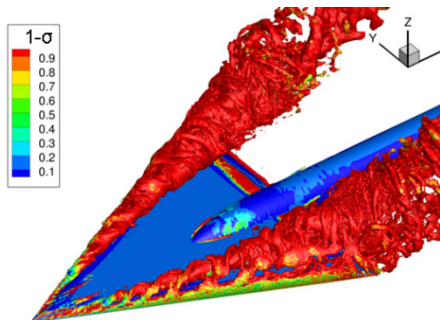

FIGURE 5. Q-criterion colored by the blending function of the HLD2 scheme for a Delta wing at $\alpha=23°$.

The grid is of hybrid type, consisting of prism layers near the surface and tetrahedra in the outer flow domain. It comprises 17 million grid points in total and is considered to meet industrial standards. Simulations with SST-based DDES were conducted, using not only the hybrid LD2 (HLD2) scheme but also the standard Reference scheme in order to analyse the numerical sensitivities. FIGURE 6 shows the coefficients of mean pressure and root-mean-square (RMS) values of the pressure fluctuations in exemplary spanwise cut sections through the surface.
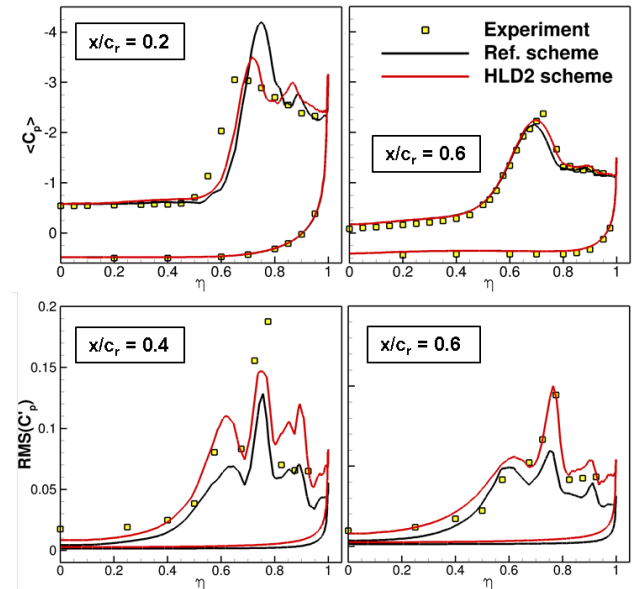

FIGURE 6. Spanwise cuts with mean pressure (top) and RMS-pressure (bottom) for the Delta wing.

Two observations can be made: first, the choice of the numerical scheme has a more pronounced effect on the fluctuation intensities than on the mean pressure – a fact that was also observed for other test cases [10]. Second, the hybrid LD2 scheme provides overall convincing agreement with the experimental results [3], despite the use of a rather quickly-generated industrial grid with unstructured elements.

4. IMPROVED PHYSICAL MODELLING

One major challenge in the robust application of hybrid RANS/LES methods is the consistent modelling of the RANS/LES interface. Here, standard methods like the original DES often face the "grey area issue", which describes a delayed development of resolved turbulent structures in the initial LES regions [6], resulting in regions of underpredicted total turbulent stress. This issue was addressed both for the non-zonal methods (e.g., DES, DDES), as well as for the embedded-LES approaches (e.g., "zonal" IDDES) in TAU.

4.1. Non-zonal grey-area mitigation

In non-zonal hybrid RANS/LES methods, "grey areas" may occur e.g. in the wake of airfoil elements [10] or in the regions just after separation, where a free shear layer is formed. One generic example for the latter is the flow over a backward-facing step. Here, typical structured grid designs contain anisotropic cells near the step corner, which are highly stretched in the spanwise direction. For

the classic DES filter-width definition $\Delta_{\max}$ used in Eq. (1), the spanwise spacing is dominant in this region, even though the flow in the initial shear layer is oriented in the plane normal to the spanwise direction. Thus, unnecessary high levels of modelled eddy-viscosity are computed which stabilize the flow and damp the development of resolved turbulence.

One promising remedy is the use of flow-adaptive filter scales, which consider only the relevant grid-spacing directions to resolve local flow gradients. In this work, we follow an approach by Chauvet et al. [1], but reformulate their purely-structured definition into a general expression that is suitable for TAU's unstructured dual-cell approach. As sketched in FIGURE 7, the surface elements $\vec{s}_i$ of each control volume are projected onto the local (normalized) vorticity vector $\vec{n}_\omega$. By summing up the contributions, the following vorticity-sensitive filter scale can be derived:

$$(3) \quad \Delta_\omega = \sqrt{\tfrac{1}{2}\sum_i |\vec{n}_\omega \cdot \vec{s}_i|} \ , \quad \text{with: } \vec{n}_\omega = \frac{\vec{\omega}}{|\vec{\omega}|} \ ,$$

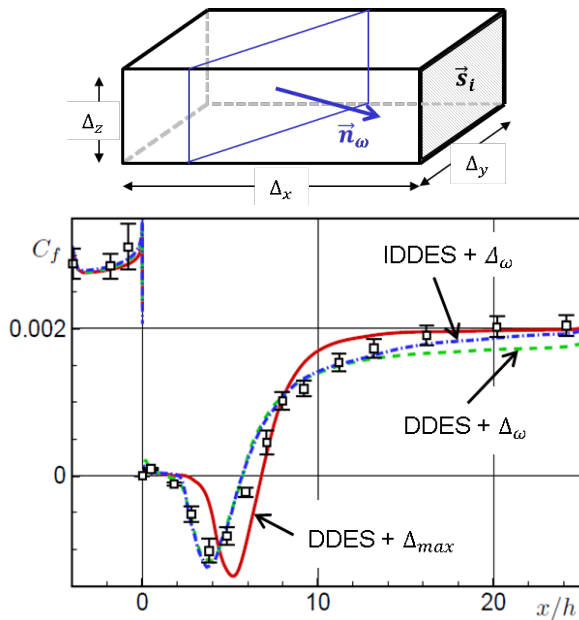which is used as Δ in Eq. (1) instead of $\Delta_{\max}$.

FIGURE 7. Sketch of a grid cell for deriving the general unstructured form of Δ_ω (top) and skin friction along a backward-facing step (bottom).

With this filter scale, the predictions of the backward-facing step flow can be significantly improved, see the skin-friction distribution in FIGURE 7. Unlike the original DDES using $\Delta_{\max}$, the recirculation region (0 < x/h < 5) computed with Δ_ω agrees well with the experiment. Moreover, the filter can be coupled with IDDES, which allows for a better prediction of the recovery region downstream of reattachment (x/h > 10).

4.2. Embedded LES - Synthetic-Eddy method

In embedded approaches, the LES region is usually fixed by the user and may comprise regions of attached wall-bounded flow. Thus, the flow through the RANS/LES interface is even more stable than in the free shear layers

or separations of non-zonal applications, so that more effective methods to augment the transition from modelled to resolved turbulence are required.

This can be accomplished by synthetic-turbulence generators, which are supposed to transform the modelled (RANS) turbulence from upstream into realistic unsteady fluctuations (LES) at the embedded interface. The minimum requirement concerning the realism of the synthetic fluctuations is the preservation of the 1st- and 2nd-order statistical moments of the RANS input in the time-averaged sense. One suitable synthetic-turbulence generator that was recently integrated in TAU is the Synthetic-Eddy Method (SEM, [1]). Note that alternative methods have also been implemented and tested [1], but this work focuses on the SEM and its variant, the Divergence-free SEM (DFSEM, [8]).

In the SEM, a discrete set of vortex elements ('synthetic eddies') are randomly placed inside a rectangular box around the plane, see the sketch in FIGURE 8. The eddies are convected at bulk velocity through the box and are re-generated at the inlet upon exiting the box, thus keeping the total eddy number constant. Their sizes and intensities are derived from the RANS input statistics, employing a Cholesky decomposition of the Reynolds stress tensor.

The DFSEM modifies some details of the SEM formulation, so that the computed velocity field fulfils the divergence-free requirement of realistic incompressible turbulence. The main benefit is a reduced generation of artificial pressure waves ('noise'), but coming at the cost of an imperfect reproduction of the anisotropic turbulent stress tensor from the RANS input [8].
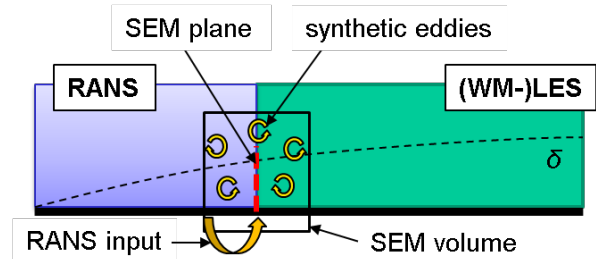

FIGURE 8. Sketch of the embedded-LES functionality in TAU using the Synthetic Eddy Method (SEM).

To transfer the induced velocity fluctuations into the actual TAU flow simulation, they can either be prescribed via a Dirichlet-type boundary condition at the inflow (*(DF)SEM-inflow*), or inserted at an arbitrary interface plane inside the flow domain using local momentum source terms (*(DF)SEM-interface*).

Both these approaches are compared for the flat-plate flow sketched in FIGURE 8, where the RANS region upstream of the interface at x/L = 0.35 is only present in the *(DF)SEM-interface* cases. To limit the required grid resolution, the resolved flow downstream the interface is treated as wall-modelled LES, by means of the IDDES.

The resulting skin-friction distributions for both SEM and DFSEM are shown in FIGURE 9. Ideally, c_f would fall monotonically along the whole plate and match the reference data from the Coles-Fernholz correlation. Instead, all simulations exhibit a sudden drop of c_f just downstream of the interface, followed by a subsequent recovery. This behaviour is typical for synthetic turbulence

methods and well in line with results from literature [8]. However, while the basic SEM appears rather insensitive to the respective setup (i.e., *SEM-inflow* or *SEM-interface*) and somewhat overpredicts the reference data after recovery, the DFSEM yields a larger adaptation distance in the *DFSEM-interface* case. Further downstream, the DFSEM results agree better with the Coles-Fernholz correlation.
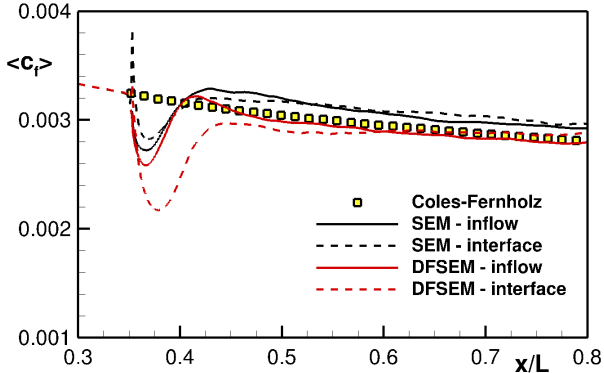

FIGURE 9. Skin friction on a flat plate computed with variants of embedded WM-LES in TAU.

With such methods at hand, the embedded approach can be applied to more practical aeronautical problems, such as the flow about the DLR-F15 3-element airfoil [17]. In this work, (WM-)LES is restricted to the critical flap region, where at higher angles of attack a pressure-induced separation emerges that limits maximum lift.

As depicted in FIGURE 10, two SEM planes are manually placed near the trailing edge of the main-wing element on both its upper and lower sides. The length-scale ratio l_{hyb}/l_{RANS} indicates the fixed RANS ($l_{hyb}/l_{RANS} = 1$) and WM-LES ($l_{hyb}/l_{RANS} < 1$) zones within the modified IDDES approach. Compared to a non-zonal reference IDDES, which was conducted on a fully-resolved structured grid with 27 million points, the embedded approach allows for a grid-point reduction of more than 60% [10].
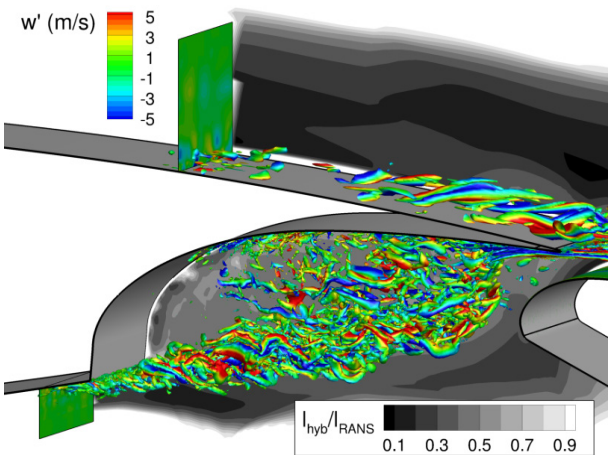

FIGURE 10. Main-wing trailing edge region of the DLR-F15 3-element airfoil, showing the embedded WM-LES setup with two SEM planes.

Time-averaged results for the global IDDES and the "zonal" IDDES with an embedded WM-LES region around the flap are compared in FIGURE 11 and FIGURE 12. The

approaches deviate just slightly in terms of the mean surface pressure (determining airfoil lift) and show a remarkably consistent skin-friction distribution and separation behaviour on the flap.

Qualitative differences are only observed in the skin friction on the main-wing element (0.2 < x/c < 0.9), where in the global IDDES the flow is resolved in WM-LES mode, whereas in the zonal IDDES the RANS mode prevails up to around x/c ≈ 0.7-0.75. In the embedded approach, both SEM interfaces exhibit only small disturbances in c_f. Overall, the embedded LES approach is shown to represent a feasible alternative to the global approach for this flow, at significantly reduced computational costs.
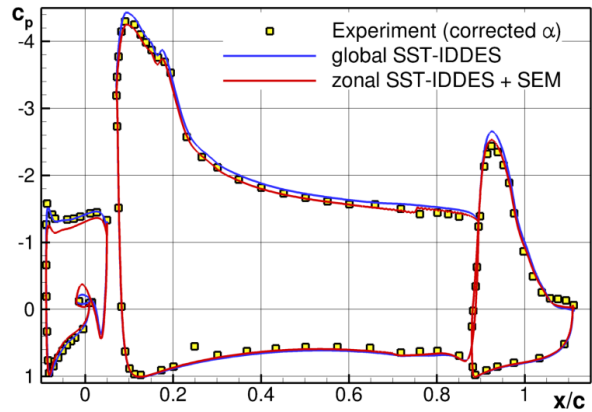

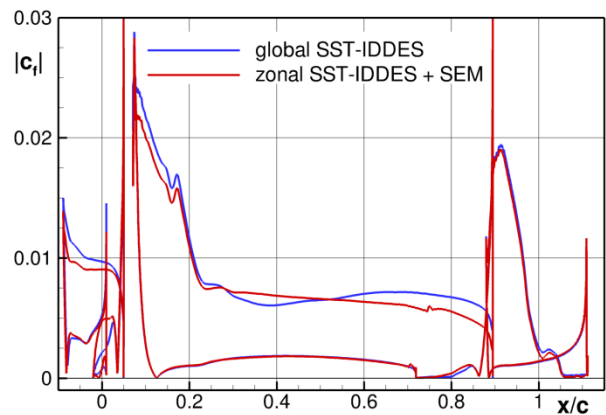FIGURE 11. Mean pressure distribution on the DLR-F15 3-element airfoil.

FIGURE 12. Mean skin-friction distribution on the DLR-F15 3-element airfoil.

5. CONCLUSION

This paper gave an overview of the recent progress in the development and application of scale-resolving simulation methods in the unstructured compressible DLR-TAU code. These include LES and hybrid RANS/LES methods.

On the one hand, numerical improvements in the form of a (hybrid) low-dissipation low-dispersion discretization scheme were presented. The new scheme allows for accurate simulations of wall-bounded flows using LES or wall-modelled LES and provides satisfying hybrid

RANS/LES predictions on unstructured meshes, as shown for the flow about a Delta wing at high incidence. On the other hand, the recent developments of physical modelling focused on the grey-area issue, which is present in both non-zonal and embedded-LES approaches. For the former, a vorticity-sensitive sub-grid filter scale was implemented, which enhances the development of turbulent structures on anisotropic meshes and was shown to improve the prediction of a backward-facing step flow. Embedded-LES applications with TAU have been realized through the implementation of the Synthetic Eddy Method, which can be used to model RANS-LES transition within attached boundary layers.

All these developments represent considerable steps in extending the capabilities of TAU's scale-resolving simulation methods towards the border of the flight envelope.

6. REFERENCES

[1] Chauvet, N., Deck, S., & Jacquin, L. (2007). Zonal Detached Eddy Simulation of a Controlled Propulsive Jet. AIAA Journal, 45(10), 2458–2473.

[2] Francois, D. G., Radespiel, R., & Probst, A. (2014). Airfoil Stall Simulation with Algebraic Delayed DES and Physically Based Synthetic Turbulence for RANS-LES Transition. In 32nd AIAA Applied Aerodynamics Conference, 16–20 June.

[3] Furman, A., & Breitsamter, C. (2009). Experimental investigations on the VFE-2 configuration at TU Munich, Germany. In Chapter 21 in: Understanding and Modeling Vortical Flows to Improve the Technology Readiness Level for Military Aircraft, RTO-TR-AVT-113, NATO RTO.

[4] Jarrin, N., Prosser, R., Uribe, J., Benhamadouche, S. and Laurence, D. (2009), Reconstruction of turbulent fluctuations for hybrid RANS/LES simulations using a synthetic-eddy method, Int. J. Heat and Fluid Flow, Vol. 30, pp. 435–442.

[5] Löwe, J., Probst, A., Knopp, T., and Kessler, R. (2015), A Low-Dissipation Low-Dispersion Second-Order Scheme for Unstructured Finite-Volume Flow Solvers, AIAA 2015-0815.

[6] Mockett, C., Haase, W., & Thiele, F. (2015). Go4Hybrid: A European initiative for improved hybrid RANS-LES modelling. In Progress in Hybrid RANS-LES Modelling. Notes on Numerical Fluid Mechanics and Multidisciplinary Design, Springer International Publishing (Vol. 130, pp. 299-303).

[7] Moser, R., Kim, J., & Mansour, N. (1999). Direct numerical simulation of turbulent channel flow up to Re = 590. Physics of Fluids, 11(4), 11–13.

[8] Poletto, R., Revell, A., Craft, T., & Jarrin, N. (2011). Divergence free synthetic eddy method for embedded LES inflow boundary conditions. In Seventh International Symposium On Turbulence and Shear Flow Phenomena (TSFP-7), Ottawa, Canada.

[9] Probst, A., & Reuß, S. (2015). Scale-Resolving Simulations of Wall-Bounded Flows with an Unstructured Compressible Flow Solver. In Progress in Hybrid RANS-LES Modelling. Notes on Numerical Fluid Mechanics and Multidisciplinary Design, Springer International Publishing (Vol. 130, pp. 481–491).

[10] Probst, A., Reuß, S., Knopp, T., & Schwamborn, D. (2015). Hybrid RANS/LES Simulations of the DLR-F15 using the DLR-TAU Code. In DLR Symposium "High-Lift System Research - celebrating 10 years of DLR-F15", 07.-09. December 2015, Braunschweig.

[11] Probst, A., Löwe, J., Reuß, S., Knopp, T. and Kessler, R. (2015), Scale-Resolving Simulations with a Low-Dissipation Low-Dispersion Second-Order Scheme for Unstructured Finite-Volume Flow Solvers, AIAA 2015-0816.

[12] Schwamborn, D., Gardner, A., von Geyr, H., Krumbein, A., Lüdeke, H., and Stürmer, A. (2008), Development of the TAU Code for Aerospace Applications, 50th NAL International Conf. on Aerospace Science & Technology, 26-28 June 2008, Bangalore. http://elib.dlr.de/55519/1/INCAST_Schwamborn.pdf

[13] Shur, M.L., Spalart, P.R., Strelets, M.Kh. and Travin, A.K. (2008), A hybrid RANS-LES approach with delayed-DES and wall-modelled LES capabilities, Int. J. Heat and Fluid Flow, Vol. 29, pp.1638-1649.

[14] Spalart, P. R., Jou, W., Strelets, M., & Allmaras, S. (1997). Comments of Feasibility of LES for Wings, and on a Hybrid RANS/LES Approach. In International Conference on DNS/LES, Ruston, Louisiana, Aug. 4-8.

[15] Spalart, P. R., Deck, S., Shur, M. L., Squires, K. D., Strelets, M. K., & Travin, A. (2006). A New Version of Detached-Eddy Simulation, Resistant to Ambiguous Grid Densities. Theoretical and Computational Fluid Dynamics, 20(3), 181–195.

[16] Travin, A., & Shur, M. (2004). Physical and Numerical Upgrades in the Detached-Eddy Simulation of Complex Turbulent Flows. Advances in LES of Complex Flows, 65(5), 239–254.

[17] Wild, J., Pott-Pollenske, M., & Nagel, B. (2006). An integrated design approach for low noise exposing high-lift devices. 3rd AIAA Flow Control Conference.